Hindawi
Advances in Civil Engineering
Volume 2018, Article ID 3729143, 10 pages
https://doi.org/10.1155/2018/3729143

Research Article

Analytical Method for Evaluating the Ground Surface Settlement Caused by Tail Void Grouting Pressure in Shield Tunnel Construction

Changsheng Wu [1,2] **and Zhiduo Zhu** [1,2]

[1] *Institute of Geotechnical Engineering, Southeast University, Nanjing 210096, China*
[2] *Jiangsu Key Laboratory of Urban Underground Engineering & Environmental Safety, Southeast University, Nanjing 210096, China*

Correspondence should be addressed to Changsheng Wu; shengchangwu@126.com

Received 14 January 2018; Revised 18 June 2018; Accepted 28 June 2018; Published 19 July 2018

Academic Editor: Li Li

The tail void grouting is a key step in shield tunnel construction and has an important influence on the loading on the surrounding soil and on the resulting settlement. In order to estimate the ground surface settlement caused by tail void grouting pressure in tunnel construction, the loading on the surrounding soil is simplified as an expansion problem of the cylindrical cavity in semi-infinite elastic space. A simple analytical formula is deduced by using the virtual image technique and Fourier transform solutions. The effectiveness of the proposed method is verified by case studies. The effects of elastic modulus, tail void grouting pressure, tunnel radius, and tunnel depth on the ground surface heave are conducted. The results indicate that the computed results are in accordance with Ye's solution and it is more rational to consider the ground surface heave induced by tail void grouting pressure in the prediction of ground settlement due to shield excavation. Moreover, the ground surface heave owing to tail void grouting pressure resembled a Gaussian distributed curve. Thus, no matter the ground surface subsidence or ground surface heave can be predicted by means of adding the presented empirical formula to the Peck formula which cannot predict the ground surface heave. The ground surface heave decreases with an increase in elastic modulus. On the contrary, as the tail void grouting pressure and tunnel radius increase, the ground surface heave increases, respectively. The ground surface heave first steadily increases and then declines gradually with the tunnel depth increase.

1. Introduction

Recently in China, there are an increasing number of tunnels under construction or being planned in order to cope with the growing demand for public and sustainable transport in heavily urbanized areas. Shield tunnel has become a well-established tunnel construction method in various ground conditions, and it is characterized by continuously applied supporting measures to stabilize the surrounding underground, to minimize surface settlements, and to prevent an inflow of the groundwater into the construction site during excavation. The tail void between the lining and the soil in a tunnel is filled with grouting during the construction of a tunnel. So tail void grouting appears to be an important process in shield tunnel and has an important influence on the resulting settlement and on the loading on the surrounding soil. A large amount of research methods for prediction surface settlement induced by the shield tunnel have been developed over these years and can be summarized in empirical methods [1–8], analytical methods [9–16], and numerical simulation [17–21]. In recent years, artificial neural network [22–24] has been developed for analysis of surface settlement caused by the shield tunnel. However, the effect of tail void grouting pressure is not taken seriously in

these methods predicting surface settlement. Some studies on tail void grouting show that the grouting pressure induced a negative settlement (i.e., soil heave) at the end of the shield mainly based on numerical simulations [25–28], laboratory tests [29–31], and field investigation [32–34]. In addition, some scholars [35–37] have made an attempt using analytical methods to analyze the surface settlement induced by tail void grouting. Numerical simulation and field measurement are still widely used; however, predictions of surface settlement caused by tail void grouting based on such methods are insufficient for most practical applications. Existing analytical methods have the shortcoming that the approximate solution can be obtained by numerical integration because these methods involve complex integrals. Besides, on the whole, there are a limited number of analytical tools that can be used to predict surface settlement induced by tail void grouting.

Hence, this paper presents an analytical methodology to predict the surface settlement of tunnels in saturated ground taking the influence of tail void grouting into account. The effect of tail void grouting pressure on the surrounding soil is simplified as an expansion problem of the cylindrical cavity in semi-infinite elastic solid. Then, a formula without complex integrals is deduced by using the virtual image technique and Fourier transform solutions. The calculation results are verified by case studies of in situ monitored surface settlement. Although the method is based on elasticity and does not fully account for the behavior of the soil, the predictions are quite good when compared with actual cases, and the solution may be used for preliminary design. Furthermore, a parametric analysis is also conducted to investigate the effects of different factors on the behaviors of the ground surface heave due to tail void grouting pressure in shield tunnel construction, including the elastic modulus, tail void grouting pressure, tunnel depth, and tunnel radius.

2. Statement of the Problem

The tail void grouting is a key step in shield tunnel construction, which has a significant influence on controlling the ground surface deformation. The grouting at shield tail void may exert radial pressure on the surrounding soil, causing the deformation of the surrounding soil. The effect of tail void grouting on the surrounding soil can be simplified as an expansion problem of the cylindrical cavity in semi-infinite elastic solid (Figure 1).

The radius of the tunnel buried at a depth h in soft clay is R. P stands for tail void grouting pressure, and the origin of the coordinate is at the ground surface above the tunnel. The basic assumptions made in developing the solutions presented in this study are stated below: (a) the soil around the tunnel is an elastic and homogeneous isotropic saturated medium and undrained conditions apply; (b) the longitudinal length of the tunnel is large enough to meet plane strain conditions; (c) the formation of grouting pressure is mainly in the cross section, and the dissipation of grouting pressure is not considered in the process of tail void grouting; and (d) the tail void is completely filled with the slurry. The penetration between soil and slurry is neglected.

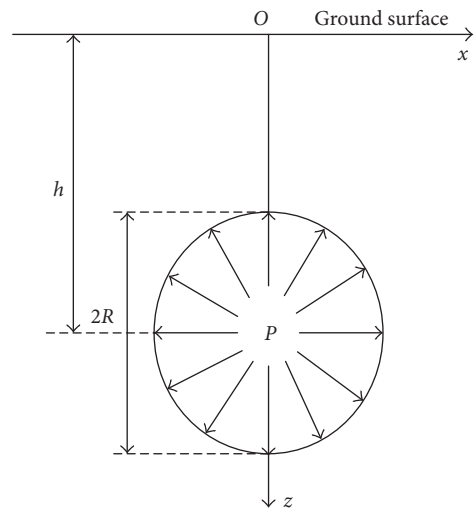

Figure 1: Cylindrical cavity expansion in semi-infinite elastic space.

3. The Analytical Solution

3.1. The Analytical Solution Steps. Based on basic assumptions, the effect of tail void grouting pressure on the surrounding soil can be simplified as an expansion problem of the cylindrical cavity in semi-infinite elastic solid. The virtual image technique proposed by Sagaseta [38] was presented for obtaining the strain field in an initially isotropic and homogeneous incompressible soil due to near-surface ground loss. The effectiveness of the virtual image technique has been verified and widely used by hundreds of scholars [10–13, 39–42]. Therefore, the virtual image technique can be used to analyze the ground surface deformation induced by tail void grouting at the shield tunnel in this work. The analysis of a problem such as that depicted in Figure 1 involves several steps, as follows (Figure 2): (a) The effect of the ground surface is neglected, and the strains are computed as the expansion of the cylindrical cavity due to tail void grouting pressure on the surrounding soil was in an infinite medium. (b) Taking a virtual positive image of the actual expansion with respect to the top surface will produce the same normal stresses and opposite shear stresses. The strains due to the virtual positive image are added to those calculated in step (a). (c) The remaining normal stresses at the surface are then evaluated and subsequently removed. The resulting strains are again added to those obtained in steps (a) and (b).

3.2. The Analytical Solution. According to step (a), the solutions of actual expansion of the cylindrical cavity in an infinite medium can be obtained based on elastic foundation theory in polar coordinates (Figure 3):

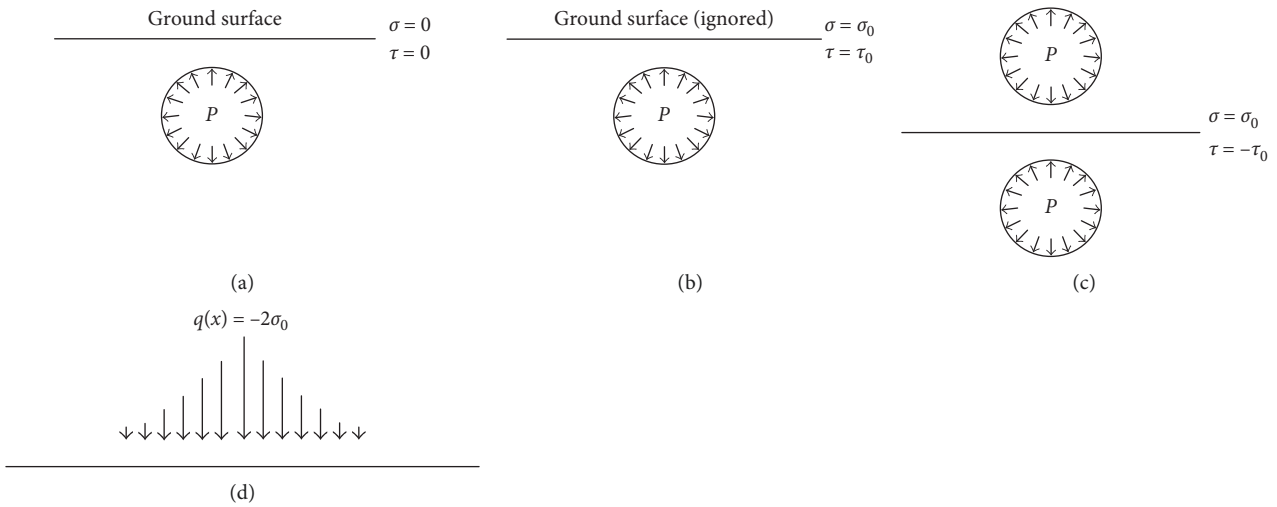

Figure 2: Steps in the analysis: (a) actual problem; (b) infinite medium; (c) positive image; (d) surface stresses.

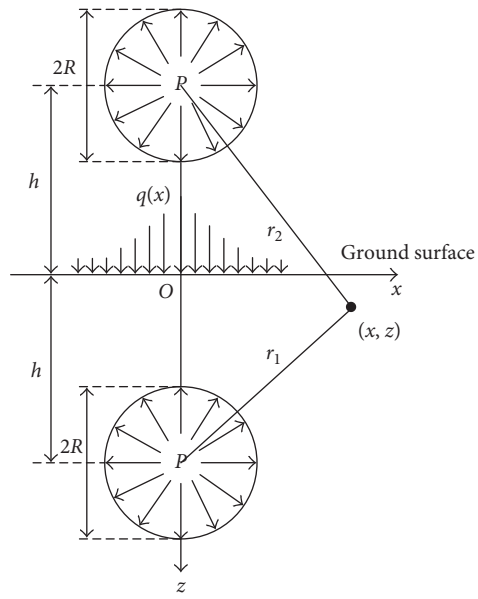

Figure 3: Modified positive stresses on the ground of cylindrical cavity expansion.

$$\sigma_{r1} = p\left(\frac{R}{r_1}\right)^2,$$

$$\sigma_{\varphi 1} = -p\left(\frac{R}{r_1}\right)^2, \tag{1}$$

$$u_{r1} = \frac{(\mu+1)pr_1}{E}\left(\frac{R}{r_1}\right)^2 = \frac{pr_1}{2G}\left(\frac{R}{r_1}\right)^2.$$

$$\sigma_{r2} = p\left(\frac{R}{r_2}\right)^2,$$

$$\sigma_{\varphi 2} = -p\left(\frac{R}{r_2}\right)^2, \tag{2}$$

$$u_{r2} = \frac{(\mu+1)pr_2}{E}\left(\frac{R}{r_2}\right)^2 = \frac{pr_2}{2G}\left(\frac{R}{r_2}\right)^2,$$

Similarly, the solutions of virtual positive image expansion based on the symmetry axis of the ground are given as follows:

where σ_{r1} and σ_{r2} are the radial stresses caused by actual expansion and virtual positive image in the infinite medium, respectively; $\sigma_{\varphi 1}$ and $\sigma_{\varphi 2}$ are the tangential stresses caused by

actual expansion and virtual positive image in the infinite medium, respectively; u_{r1} and u_{r2} are the radial deformation caused by actual expansion and virtual positive image in the infinite medium, respectively; p is the expansion pressure of the cylindrical cavity in an infinite medium, which is the difference between grouting pressure and initial total stresses; R is the excavation radius of the shield tunnel; r_1 and r_2 are the distance from the arbitrary point in soil to the actual, virtual positive image expansion centerline and can be expressed as $r_1 = \sqrt{(z-h)^2 + x^2}$ and $r_2 = \sqrt{(z+h)^2 + x^2}$, respectively, in which x and z are the coordinates with origin at the ground surface above the tunnel and h is the depth from the ground surface to the tunnel centerline; and μ, E, and G denote the Poisson ratio, the elastic modulus, and the shear modulus of the soil, respectively.

Then, from (1) and (2), it can be obtained by converting the polar coordinate system into the rectangular coordinate system that

$$\begin{aligned}
\sigma_{x0} &= pR^2\left[\frac{x^2}{r_1^4} - \frac{(z-h)^2}{r_1^4} + \frac{x^2}{r_2^4} - \frac{(z+h)^2}{r_2^4}\right],\\
\sigma_{z0} &= pR^2\left[\frac{(z-h)^2}{r_1^4} - \frac{x^2}{r_1^4} + \frac{(z+h)^2}{r_2^4} - \frac{x^2}{r_2^4}\right],\\
\tau_{xz0} &= 2pR^2\left[\frac{x(z-h)}{r_1^4} + \frac{x(z+h)}{r_2^4}\right],\\
u_{x0} &= \frac{pR^2}{2G}\left(\frac{x}{r_1^2} + \frac{x}{r_2^2}\right),\\
u_{z0} &= \frac{pR^2}{2G}\left(\frac{z-h}{r_1^2} + \frac{z+h}{r_2^2}\right)^2,
\end{aligned} \tag{3}$$

where σ_{x0}, σ_{z0}, and τ_{xz0} are the horizontal stress, vertical stress, and shear stress in plane x-z, respectively, and u_{x0} and u_{z0} are the horizontal displacements and vertical displacements, respectively.

The same normal stresses and opposite shear stresses are produced at the ground surface in the first two steps, thus violating the stress-free condition. Then, substituting $z = 0$ and $r_1 = r_2$ into (3), we can obtain the normal stresses at the ground surface:

$$\sigma_{z=0} = q(x) = 2pR^2\frac{h^2 - x^2}{(h^2 + x^2)^2}. \tag{4}$$

In order to meet the free-surface condition, the opposite normal stresses should be acted on the ground surface (Figure 3). This problem can be solved by displacement analytical solution based on elastic theory. The equilibrium differential equation expressed with the displacement component of plane strain is

$$\begin{aligned}
\frac{2(1-\mu)}{1-2\mu}\frac{\partial^2 u_{x3}}{\partial x^2} + \frac{\partial^2 u_{x3}}{\partial z^2} + \frac{1}{1-2\mu}\frac{\partial^2 u_{z3}}{\partial x \partial z} &= 0,\\
\frac{2(1-\mu)}{1-2\mu}\frac{\partial^2 u_{z3}}{\partial z^2} + \frac{\partial^2 u_{z3}}{\partial x^2} + \frac{1}{1-2\mu}\frac{\partial^2 u_{x3}}{\partial x \partial z} &= 0,
\end{aligned} \tag{5}$$

where u_{x3} and u_{z3} are the horizontal displacements and vertical displacements owing to the opposite normal stresses, respectively.

The boundary conditions can be described as follows:

$$\begin{aligned}
\tau_{xz}\big|_{z=0} &= \frac{E}{2(1+\mu)}\left(\frac{\partial u_{z3}}{\partial x} + \frac{\partial u_{x3}}{\partial z}\right) = 0,\\
\sigma_z\big|_{z=0} &= \frac{(1-\mu)E}{(1+\mu)(1-2\mu)}\left(\frac{\partial u_{z3}}{\partial z} + \frac{\mu}{1-\mu}\frac{\partial u_{x3}}{\partial x}\right) = q(x).
\end{aligned} \tag{6}$$

In order to avoid the complex integrals, the equation can be solved with the Fourier transform [43]. According to Fourier transforms properties, the functions are given as below:

$$u_{x3} = \int_0^\infty U_{x3}(\omega, z)\sin\omega x\, d\omega, \tag{7}$$

$$u_{z3} = \int_0^\infty U_{z3}(\omega, z)\cos\omega x\, d\omega, \tag{8}$$

$$\begin{aligned}
F\left(\frac{\partial^2 u_{x3}}{\partial x^2}\right) &= -\omega^2 U_{x3}(\omega, z),\\
F\left(\frac{\partial^2 u_{x3}}{\partial z^2}\right) &= \frac{\partial^2}{\partial z^2}U_{x3}(\omega, z),
\end{aligned} \tag{9}$$

where U_{x3} and U_{z3} are the Fourier transforms formulas of u_{x3} and u_{z3}, respectively; F stands for Fourier transform; and ω is the Fourier transform parameter.

Then, the equilibrium differential equations (5) after Fourier transform are obtained:

$$\begin{aligned}
-\frac{2(1-\mu)}{1-2\mu}\omega^2 U_{x3} + \frac{\partial^2 U_{x3}}{\partial z^2} - \frac{\omega}{1-2\mu}\frac{\partial U_{z3}}{\partial z} &= 0,\\
\frac{2(1-\mu)}{1-2\mu}\frac{\partial^2 U_{z3}}{\partial z^2} - \omega^2 U_{z3} + \frac{\omega}{1-2\mu}\frac{\partial U_{x3}}{\partial z} &= 0.
\end{aligned} \tag{10}$$

Similarly, the boundary conditions (6) are given as below:

$$\begin{aligned}
F(\tau_{xz})\big|_{z=0} &= \frac{E}{2(1+\mu)}\left(-\omega U_{z3} + \frac{\partial U_{x3}}{\partial z}\right) = 0,\\
F(\sigma_z)\big|_{z=0} &= \frac{(1-\mu)E}{(1+\mu)(1-2\mu)}\left(\frac{\partial U_{z3}}{\partial z} + \frac{\mu}{1-\mu}\omega U_{x3}\right)\\
&= F[q(x)].
\end{aligned} \tag{11}$$

The general solution of (10) is

$$\begin{aligned}
U_{x3} &= \left(A + \frac{\omega z B}{1-2\mu}\right)e^{\omega z},\\
U_{z3} &= \left[-A + \frac{(3-4\mu-\omega z)}{1-2\mu}B\right]e^{\omega z},
\end{aligned} \tag{12}$$

where A and B are the undetermined coefficients.

Substituting (12) into (11), the following equations can be obtained:

$$A = B, \tag{13}$$

$$\frac{\omega E}{(1+\mu)(1-2\mu)} A = F[q(x)]. \tag{14}$$

According to the definition of Fourier transform,

$$F[q(x)] = \frac{2}{\pi} \int_0^\infty q(x) \cos \omega x \, dx. \tag{15}$$

The undetermined coefficient A can be calculated by combining (14) and (15):

$$A = \frac{2(1+\mu)(1-2\mu)}{\pi \omega E} \int_0^\infty q(x) \cos \omega x \, dx. \tag{16}$$

Substituting (4) into (16), the undetermined coefficient A can be obtained on the basis of well-known Bateman integral [44]:

$$\begin{aligned} A &= \frac{2(1+\mu)(1-2\mu)}{\pi \omega E} \int_0^\infty 2pR^2 \frac{h^2 - x^2}{h^2 + x^2} \cos \omega x \, dx, \\ &= \frac{4(1+\mu)(1-2\mu)pR^2}{\pi \omega E} \times \frac{\pi \omega}{2} e^{-\omega h}, \\ &= \frac{2(1+\mu)(1-2\mu)pR^2}{E} e^{-\omega h}. \end{aligned} \tag{17}$$

Combining (7), (8), (12), (13), and (17), u_{x3} and u_{z3} can be expressed as follows:

$$\begin{aligned} u_{x3} &= \int_0^\infty A \left(1 + \frac{\omega z}{1-2\mu}\right) e^{\omega z} \sin \omega x \, d\omega \\ &= 2pR^2 \times \frac{(1+\mu)(1-2\mu)}{E} \\ &\quad \cdot \int_0^\infty \left[1 + \frac{z\omega}{(1-2\mu)}\right] e^{\omega(z-h)} \sin \omega x \, d\omega, \\ &= \frac{2(1+\mu)(1-2\mu)pR^2}{E} \\ &\quad \times \left[\frac{x}{(h-z)^2 + x^2} + \frac{z}{1-2\mu} \frac{2(h-z)x}{(h-z)^2 + x^2}\right], \end{aligned} \tag{18}$$

$$\begin{aligned} u_{z3} &= \int_0^\infty A \left(1 + \frac{1-\omega z}{1-2\mu}\right) e^{\omega z} \cos \omega x \, d\omega \\ &= 2pR^2 \times \frac{(1+\mu)(1-2\mu)}{E} \\ &\quad \cdot \int_0^\infty \left(1 + \frac{1-\omega z}{1-2\mu}\right) e^{\omega(z-h)} \cos \omega x \, d\omega, \\ &= \frac{2(1+\mu)(1-2\mu)pR^2}{E} \\ &\quad \times \left\{\frac{2(1-\mu)}{1-2\mu} \frac{h}{(h-z)^2 + x^2} - \frac{z}{1-2\mu} \frac{(h-z)^2 - x^2}{\left[(h-z)^2 + x^2\right]^2}\right\}. \end{aligned} \tag{19}$$

The final displacement expressions caused by tail void grouting pressure in semi-infinite soft clay for a shield tunnel are then obtained from (3), (18), and (19):

$$\begin{aligned} u_x &= u_{x0} + u_{x3}, \\ u_z &= u_{z0} + u_{z3}, \end{aligned} \tag{20}$$

where u_x and u_z are the horizontal displacements and vertical displacements induced by the expansion of the cylindrical cavity in semi-infinite soft clay soil, respectively.

The vertical displacements are generally of a greater concern than the horizontal displacements in the process of tail void grouting at shield tunnel construction. Accordingly, the vertical displacements of the ground surface can be obtained from (20) with $z = 0$:

$$u_z = u_{z3} = \frac{4(1-\mu^2)pR^2}{E} \frac{h}{h^2 + x^2}. \tag{21}$$

Furthermore, the maximum vertical displacements of the ground surface owing to tail void grouting pressure in shield tunnel construction can be obtained from (21) with $x = 0$:

$$u_{z\max} = \frac{4(1-\mu^2)pR^2}{Eh}. \tag{22}$$

3.3. The Modified Vertical Displacements. In the actual construction of the shield tunnel, the pressure effect of tail void grouting on the surrounding soil is intermittent. In addition, the vertical displacements are related to the distance away from the position of grouting pressure acting on the surrounding soil. So modified coefficient of vertical displacements can be acquired according to the method presented by Sagaseta [45] and Wei and Xu [46]:

$$\beta = \frac{(h-z-R)^2}{2\left[\sqrt{x^2 + (h-z)^2} + R\right]^2}. \tag{23}$$

Hence, the modified vertical displacements of the ground surface caused by tail void grouting pressure can be given as below with $z = 0$:

$$u_z = \beta u_{z3} = \frac{(h-R)^2}{2\left(\sqrt{x^2 + h^2} + R\right)^2} u_{z3}. \tag{24}$$

Moreover, the maximum vertical displacements of the ground surface can be obtained:

$$u_{z\max} = \frac{(h-R)^2}{2(h+R)^2} \frac{4(1-\mu^2)pR^2}{Eh}. \tag{25}$$

4. Case Studies

4.1. Case Study 1. To investigate the rationality of the presented solutions, the prediction of the presented analytic solution is compared with Ye's solution [36]. This case study proposed by Ye et al. [36] is adopted, and the parameters of the shield tunnel construction are given as follows: the radius of the shield tunnel is $R = 3.2$ m, the depth from the ground

surface to the tunnel centerline is $h = 10$ m, the initial total stress is $P_0 = 0.24$ MPa, the elastic modulus of soil is $E = 4.03$ MPa, the Poisson ratio of soil is $\nu = 0.5$, the tail void grouting pressure is $P_g = 0.30$ MPa, and the cohesive force and internal friction angle of soil are $c = 0.006$ MPa and $\varphi = 18^\circ$, respectively. For more information of this study, refer [36]. Substituting the relevant parameters into (24), the vertical displacements of the ground surface induced by tail void grouting pressure in shield tunnel construction can be obtained. The calculated results and Gauss fitting results are illustrated in Figure 4. The presented results are compared with Ye's results.

From Figure 4, tail void grouting pressure can make the ground surface heave. The results given by the presented method are in good agreement with Ye's results. However, the results obtained with the presented solution are a little larger than Ye's results. It could be attributed to the fact that Ye's solution is obtained by numerical integration resulting in approximate results. In this work, closed-form analytical solution is performed. In addition, the ground surface heave induced by tail void grouting pressure from the presented method and Ye's method are both well fitted by the Gaussian relation.

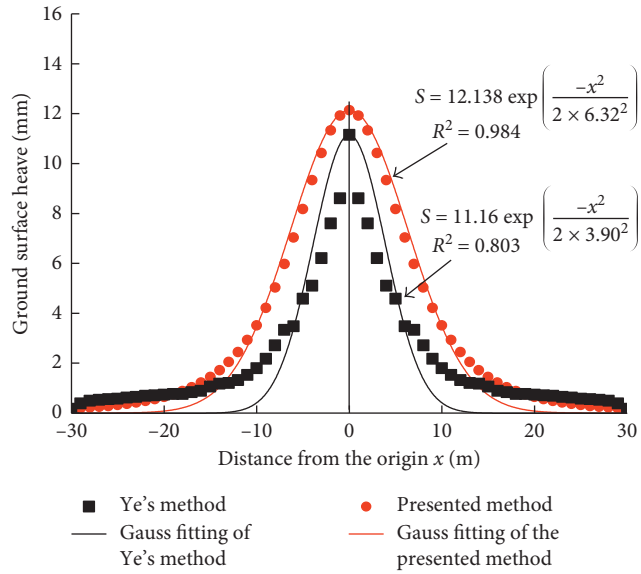

Figure 4: Ground surface heave caused by tail void grout pressure.

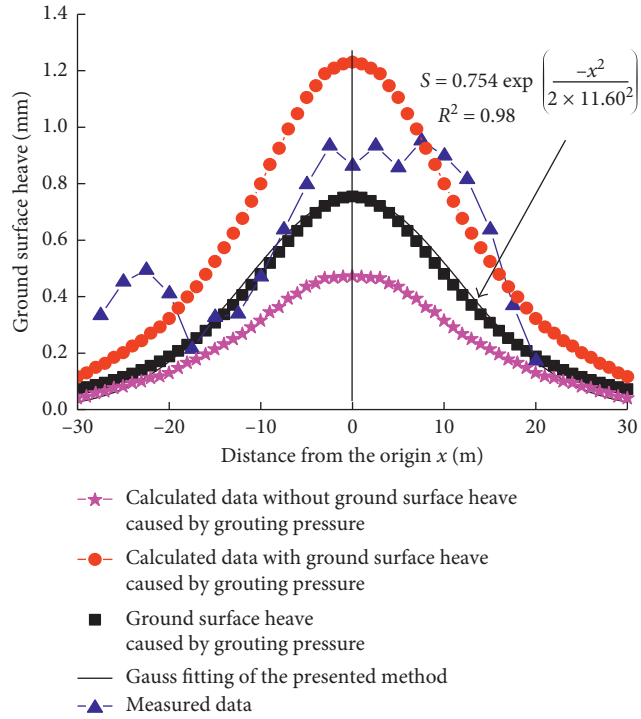

Figure 5: Ground surface settlement caused by the shield tunnel.

4.2. Case Study 2. A research site is chosen within the Channel Tunnel Rail Link Contract 250 (C250), which covers the construction of 5.2 km of twin bored tunnels of 8.126 m cut diameter between Ripple Road, Dagenham, and Barrington Road, Newham, to the east of London in Essex. The site, being built on only superficially with small nearby buildings, is considered to represent essentially greenfield conditions. At the instrumented site, tunnelling takes place through about 12.5 m London Clay using the earth pressure balance machines mode. Tunnel axes are at 18.9 m below the ground level, and the diameter of the shield is 8.126 m, with an overcutting bead of 19 mm thickness. Lining rings are assembled and erected within the shield, which is 10 m long. The nominal 0.155 m annulus left between the lining and the excavated soil profile is filled by tail void grouting using a sand grout of proportions. The initial total stresses and tail void grouting pressure are 0.34 MPa and 0.38 MPa, respectively. The elastic modulus and Poisson ratio are 29 MPa and 0.5. The parameters for the site stratigraphy, plan of the ground instrumentation, and other information are proposed by Standing and Selemetas [47]. Substituting the relevant parameters into (24), the vertical displacements of the ground surface owing to tail void grouting pressure in the shield tunnel construction can be obtained. The ground surface heave caused by tail void grouting using the presented method and Gauss fitting result is shown in Figure 5. Besides, the comparison of the results between measured data and predicted data without/with the ground surface heave caused by tail void grouting pressure is made in Figure 5. It is noted that the predicted data without ground surface heave caused by tail void grouting pressure are proposed by Liang et al. [37]. The pressures induced by the compressing effect of cutter head, the skin frictions along the shield, and the soil movements caused by volume loss are considered in his study on the basis of the Mindlin solution. The predicted data with the ground surface heave caused by tail void grouting pressure are obtained by superimposing the results of this study and those of Liang et al. [37].

As shown in Figure 5, we can confirm that tail void grouting pressure can indeed make the ground surface heave and the analytical solution heave resembles a Gauss probability function. Referring to Figure 5, the measured data of ground surface settlement are much larger than the

predicted data without taking the ground surface heave caused by tail void grouting pressure into consideration and less than the predicted data by taking the ground surface heave caused by tail void grouting pressure into consideration. From the former phenomenon, if the ground surface heave caused by tail void grouting pressure is ignored, the ground surface settlement will be underestimated, resulting in serious consequences. The reason for the latter phenomenon may be that the space occupied by the shield and lining is ignored in theoretical calculation. On the whole, the ground surface settlement caused by shield tunnel construction can be better predicted by taking the ground surface heave by the presented method into consideration, and the prediction data can be in good agreements with the measured data.

4.3. Results and Discussion. From the two case studies, the ground surface heave caused by tail void grouting pressure using the presented method can be in good agreement with the Gauss probability function. Referring to the Peck formula, we can define i_g as the horizontal distance from the tunnel centerline to the point of inflection on the surface heave trough induced by tail void grouting pressure. Then, the empirical formulas for prediction of the ground surface heave induced by tail void grouting pressure can be obtained:

$$S_g = S_{gmax} \exp\left(\frac{-x^2}{2i_g^2}\right), \tag{26}$$

where S_g is the ground surface heave caused by tail void grouting pressure, S_{gmax} is the maximum ground surface heave caused by tail void grouting pressure above the tunnel centerline, and x is the horizontal distance from the tunnel centerline. To make up the limitation in predicting the ground surface heave of the Peck formula, the empirical formulas for prediction of the ground surface heave induced by tail void grouting pressure can be added with the Peck formula which cannot predict the ground surface heave. Thus, no matter the ground surface subsidence or ground surface heave can be predicted in this way.

5. Parametric Analysis

In the previous section, the effectiveness of the proposed method has been validated by comparison with two selected case histories for the problem of the ground surface heave induced by tail void grouting pressure. In this section, in order to investigate the influences of different parameters on the ground surface heave caused by tail void grouting pressure, taking Channel Tunnel Rail Link Contract 250 (C250) as an example, a series of parametric analyses are carried out on the basis of (24). The influences of the elastic modulus, tail void grouting pressure, tunnel radius, and tunnel depth are considered and analyzed. It is noted that, in analysis for investigating the effects of each parameter, the value of one parameter is changed, while the other parameters are kept constant as those in case study 2. The results are shown in Figure 6.

Referring to Figure 6, it can be seen that all the curves have similar heave patterns and points located above the tunnel centerline have a bigger ground surface heave than the other points. The ground surface heave decreases with an increase in elastic modulus. On the contrary, as the tail void grouting pressure and tunnel radius increase, the ground surface heave increases, respectively. The interesting finding is that the ground surface heave first steadily increases and then declines gradually with the tunnel depth increase. After the tunnel depth is more than 2D (D=2R), the effect of grouting pressure on the ground surface will weaken gradually. This can be responsible for the interesting finding. Furthermore, by increasing the elastic modulus from 1 MPa to 30 MPa, the ground surface heave sharply decreases. This is because the ground with larger values of elastic modulus possesses greater ground stiffness, and hence, it will significantly reduce the ground surface heave in the tunnel. In addition, it is found that the ground surface heave does not change much when tunnel radius is greater than 6 m.

6. Conclusions

The effect of tail void grouting pressure on the surrounding soil is simplified as an expansion problem of the cylindrical cavity in semi-infinite elastic space. An analytical method using the virtual image technique and Fourier transform solutions is proposed to estimate the ground surface settlement caused by tail void grouting pressure in shield tunnel construction. Closed-form solution without high complex integrals and numerical integration has been obtained taking some assumptions as a basis. Two case histories are used to verify the effectiveness of the proposed method. The computed results are in general agreement with Ye's solution and measured observations. In addition, it is found that the application of Gaussian probability function can be extended to estimate the ground surface heave due to tail void grouting pressure in shield tunnel construction. Thus, the empirical formulas for prediction of the ground surface heave induced by tail void grouting pressure can be added to the Peck formula which cannot predict the ground surface heave. In this way, not only the ground surface subsidence but also the ground surface heave can be predicted. Furthermore, a parametric analysis is also conducted to investigate the effects of different factors on the behaviors of the ground surface heave due to tail void grouting pressure in shield tunnel construction, including elastic modulus, the tail void grouting pressure, tunnel radius, and tunnel depth. The ground surface heave decreases with an increase in elastic modulus. On the contrary, as the tail void grouting pressure and tunnel radius increase, the ground surface heave increases, respectively. The ground surface heave first steadily increases and then declines gradually with the tunnel depth increase. The ground surface heave does not change much when tunnel radius is greater than 6 m.

Finally, it is suggested that further studies should be performed to investigate the accuracy of new equation.

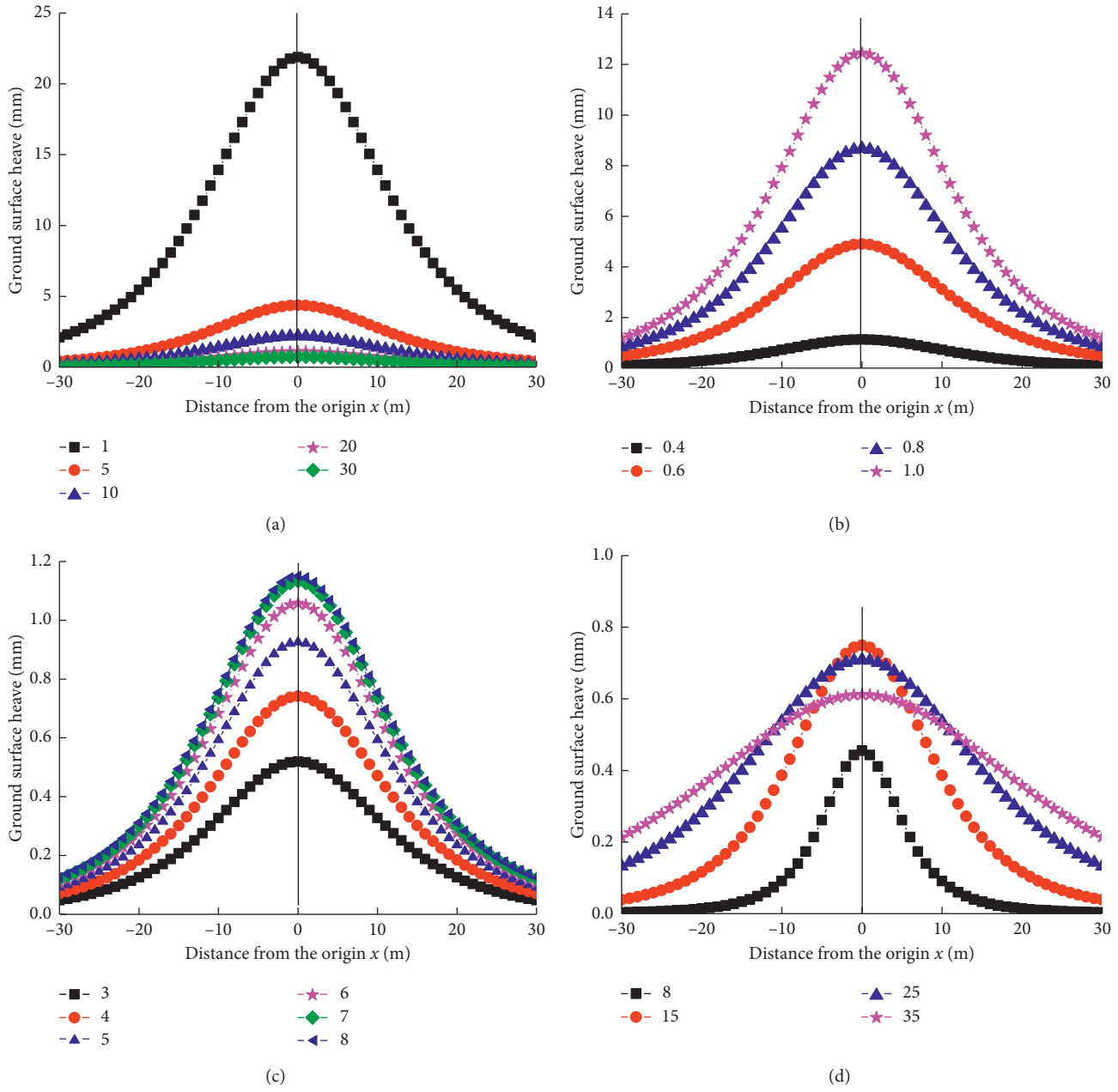

FIGURE 6: Relationship between the ground surface heave and (a) elastic modulus (MPa); (b) tail void grouting pressure (MPa); (c) tunnel radius (m); (d) tunnel depth (m).

Data Availability

The data used to support the findings of this study are available from the corresponding author upon request.

Conflicts of Interest

The authors declare that there are no conflicts of interest.

Acknowledgments

The authors would like to acknowledge the financial support from the National Program on Key Basic Research Project of China (973 Program) (2015CB057803). The authors would also like to acknowledge the contributions of Mr. Fenglei Tan, the postgraduate student of Southeast University.

Supplementary Materials

Supplementary Datasheet 1 lists original data of case study 1 (Figure 4) calculated by Ye's method and presented method, respectively. Supplementary Datasheet 2 lists calculated data and measured data of case study 2 (Figure 5) in the paper. Supplementary Datasheet 3 lists the parametric analysis (Figure 6) of the ground surface heave caused by tail void grouting pressure in shield tunnel construction. (*Supplementary Materials*)

References

[1] P. B. Peck, "Deep excavations and tunneling in soft ground," in *Proceedings of the 7th International Conference on Soil Mechanics and Foundation Engineering*, pp. 225–290, Mexico City, Mexico, 1969.

[2] P. B. Attewell and I. W. Farmer, "Ground disturbance caused by shield tunnelling in stiff, overconsolidated clay," *Engineering Geology*, vol. 8, no. 4, pp. 361–381, 1974.

[3] M. P. O'Reilly and B. M. New, "Settlements above tunnels in the United Kingdom—their magnitude and prediction," in *Proceedings of the Tunnel Conference*, pp. 173–181, Brighton, UK, 1982.

[4] R. J. Mair, "Geotechnical aspects of soft-ground tunnelling," in *Proceedings Conference on Construction Problems in Soft Soils*, Singapore, 1983.

[5] K. Y. Lo and R. K. Rowe, "Predicting settlement due to tunnelling in clay," in *ASCE, Geotechnics Conference, Tunnelling in Soil and Rock*, pp. 46–76, Atlanta, GA, USA, 2010.

[6] X. Li and X. Chen, "Using grouting of shield tunneling to reduce settlements of overlying tunnels: case study in Shenzhen metro construction," *Journal of Construction Engineering and Management*, vol. 138, no. 4, pp. 574–584, 2012.

[7] D. Dias and R. Kastner, "Movements caused by the excavation of tunnels using face pressurized shields—analysis of monitoring and numerical modeling results," *Engineering Geology*, vol. 152, no. 1, pp. 17–25, 2013.

[8] Y. S. Fang, C. T. Wu, S. F. Chen, and C. Liu, "An estimation of subsurface settlement due to shield tunneling," *Tunnelling and Underground Space Technology*, vol. 44, pp. 121–129, 2014.

[9] G. W. Clough and B. Schmidt, "Design and performance of excavations and tunnels in soft clay," *Developments in Geotechnical Engineering*, vol. 20, pp. 567–634, 1981.

[10] A. Verruijt and J. R. Booker, "Surface settlements due to deformation of a tunnel in an elastic half plane," *Géotechnique*, vol. 46, no. 4, pp. 753–756, 1996.

[11] N. Loganathan and H. G. Poulos, "Analytical prediction for tunneling induced ground movements in clay," *Journal of Geotechnical and Geoenvironmental Engineering*, vol. 124, no. 9, pp. 846–856, 1998.

[12] C. González and C. Sagaseta, "Patterns of soil deformations around tunnels. Application to the extension of Madrid Metro," *Computers and Geotechnics*, vol. 28, no. 6-7, pp. 445–468, 2001.

[13] A. Bobet, "Analytical solutions for shallow tunnels in saturated ground," *Journal of Engineering Mechanics*, vol. 127, no. 12, pp. 1258–1266, 2001.

[14] W. I. Chou and A. Bobet, "Predictions of ground deformations in shallow tunnels in clay," *Tunnelling and Underground Space Technology*, vol. 17, no. 1, pp. 3–19, 2002.

[15] K. H. Park, "Elastic solution for tunneling-induced ground movements in clays," *International Journal of Geomechanics*, vol. 4, no. 4, pp. 310–318, 2004.

[16] K. H. Park, "Analytical solution for tunnelling-induced ground movement in clays," *Tunnelling and Underground Space Technology*, vol. 20, no. 3, pp. 249–261, 2005.

[17] R. K. Rowe, K. Y. Lo, and G. J. Kack, "A method of estimating surface settlement above tunnels constructed in soft ground," *Canadian Geotechnical Journal*, vol. 20, no. 1, pp. 11–22, 1983.

[18] K. M. Lee, R. K. Rowe, and K. Y. Lo, "Subsidence owing to tunnelling. I. Estimating the gap parameter," *Canadian Geotechnical Journal*, vol. 29, no. 6, pp. 929–940, 1992.

[19] T. Kasper and G. Meschke, "A 3D finite element simulation model for TBM tunnelling in soft ground," *International Journal for Numerical and Analytical Methods in Geomechanics*, vol. 28, no. 14, pp. 1441–1460, 2004.

[20] T. Kasper and G. Meschke, "A numerical study of the effect of soil and grout material properties and cover depth in shield tunnelling," *Computers and Geotechnics*, vol. 33, no. 4-5, pp. 234–247, 2006.

[21] H. Chakeri, Y. Ozcelik, and B. Unver, "Effects of important factors on surface settlement prediction for metro tunnel excavated by EPB," *Tunnelling and Underground Space Technology*, vol. 36, pp. 14–23, 2013.

[22] J. Shi, J. A. R. Ortigao, and J. Bai, "Modular neural networks for predicting settlements during tunneling," *Journal of Geotechnical and Geoenvironmental Engineering*, vol. 124, no. 5, pp. 389–395, 1998.

[23] S. Suwansawat and H. H. Einstein, "Artificial neural networks for predicting the maximum surface settlement caused by EPB shield tunneling," *Tunnelling and Underground Space Technology*, vol. 21, no. 2, pp. 133–150, 2006.

[24] I. Ocak and S. E. Seker, "Calculation of surface settlements caused by EPBM tunneling using artificial neural network, SVM, and Gaussian processes," *Environmental Earth Sciences*, vol. 70, no. 3, pp. 1263–1276, 2013.

[25] F. Nagel and G. Meschke, "Grout and bentonite flow around a TBM: computational modeling and simulation-based assessment of influence on surface settlements," *Tunnelling and Underground Space Technology*, vol. 26, no. 3, pp. 445–452, 2011.

[26] L. Teng and H. Zhang, "Meso-macro analysis of surface settlement characteristics during shield tunneling in sandy cobble ground," *Rock and Soil Mechanics*, vol. 33, pp. 1141–1150, 2012, in Chinese.

[27] G. Mollon, D. Dias, and A. H. Soubra, "Probabilistic analyses of tunneling-induced ground movements," *Acta Geotechnica*, vol. 8, no. 2, pp. 181–199, 2013.

[28] J. Y. Oh and M. Ziegler, "Investigation on influence of tail void grouting on the surface settlements during shield tunneling using a stress-pore pressure coupled analysis," *KSCE Journal of Civil Engineering*, vol. 18, no. 3, pp. 803–811, 2014.

[29] Y. Koyama, N. Okano, Y. Sato, and M. Shimizu, *Back-Fill Grouting Model Test for Shield Tunnel*, Railway Technical Research Institute, Kokubunji, Japan, 1998.

[30] T. Kasper and G. Meschke, "On the influence of face pressure, grouting pressure and TBM design in soft ground tunnel," *Tunnelling and Underground Space Technology*, vol. 21, no. 2, pp. 160–171, 2006.

[31] S. Cavalaro and A. Aguado, "Characterization of backfill mortars used in different tunnels in Spain," *Materiales de Construcción*, vol. 63, no. 309, pp. 65–78, 2013.

[32] K. Komiya, K. Soga, H. Akagi et al., "Soil consolidation associated with grouting during shield tunnelling in soft clayey ground," *Géotechnique*, vol. 51, no. 10, pp. 835–846, 2001.

[33] A. Bezuijen, A. M. Talmon, F. J. Kaalberg, and R. Plugge, "Field measurements of grout pressures during tunneling of the Sophia Rail tunnel," *Soils and Foundations*, vol. 44, no. 1, pp. 39–48, 2008.

[34] A. M. Talmon and A. Bezuijen, "Simulating the consolidation of TBM grout at Noordplaspolder," *Tunnelling and Underground Space Technology*, vol. 24, no. 5, pp. 493–499, 2009.

[35] C. G. Lin, Z. M. Zhang, S. M. Wu et al., "Study of ground heave and subsidence induced by shield tunnelling in soft ground," *Chinese Journal of Rock Mechanics and Engineering*, vol. 30, pp. 2583–2590, 2011, in Chinese.

[36] F. Ye, C. F. Gou, Z. Chen et al., "Ground surface deformation caused by synchronous grouting of shield tunnels," *Chinese*

Journal of Geotechnical Engineering, vol. 36, pp. 618–624, 2014, in Chinese.

[37] R. Z. Liang, T. D. Xia, C. G. Lin et al., "Analysis of ground surface displacement and horizontal movement of deep soils induced by shield advancing," *Chinese Journal of Mechanical Engineering*, vol. 34, pp. 583–593, 2015, in Chinese.

[38] C. Sagaseta, "Analysis of undrained soil deformation due to ground loss," *Géotechnique*, vol. 37, no. 3, pp. 301–320, 1987.

[39] C. W. W. Ng, T. L. Y. Yau, J. H. M. Li, and W. H. Tang, "New failure load criterion for large diameter bored piles in weathered geomaterials," *Journal of Geotechnical and Geoenvironmental Engineering*, vol. 127, no. 6, pp. 488–498, 2001.

[40] D. J. White and M. D. Bolton, "Displacement and strain paths during plane-strain model pile installation in sand," *Géotechnique*, vol. 54, no. 6, pp. 375–397, 2004.

[41] G. Mollon, D. Dias, A. H. Soubra, and A.-H. Soubra, "Face stability analysis of circular tunnels driven by a pressurized shield," *Journal of Geotechnical and Geoenvironmental Engineering*, vol. 136, no. 1, pp. 215–229, 2010.

[42] P. Ni, S. Mangalathu, G. Mei, and Y. Zhao, "Permeable piles: an alternative to improve the performance of driven piles," *Computers and Geotechnics*, vol. 84, pp. 78–87, 2017.

[43] M. N. Wang, *Equations of Mathematical Physics*, Tsinghua University Press, Beijing, China, 2009.

[44] H. Bateman, *Nonlinear Partial Differential Equations*, McGraw-Hill, New York, NY, USA, 2012.

[45] C. Sagaseta, "Discussion: analysis of undrained soil deformation due to ground loss," *Geotechnique*, vol. 38, no. 4, pp. 647–649, 1988.

[46] G. Wei and R. Q. Xu, "Prediction of longitudinal ground deformation due to tunnel construction with shield in soft soil," *Chinese Journal of Geotechnical Engineering*, vol. 27, pp. l077–l081, 2005, in Chinese.

[47] J. R. Standing and D. Selemetas, "Greenfield ground response to EPBM tunnelling in London Clay," *Geotechnique*, vol. 63, no. 12, pp. 989–1007, 2013.